

# Monte Carlo Implementations of Diffraction at HERA <sup>1</sup>

H. Jung

*Physics Department, Lund University, P.O. Box 118, 221 00  
Lund, Sweden*

## Abstract

**Abstract** The Monte Carlo implementation of different approaches for diffractive scattering in  $e - p$  collisions (resolved  $P$ , pQCD, soft color interactions) is described, with emphasis on the construction of the hadronic final state. Simple models for proton dissociation and exclusive vector meson production are described. A comparison of the different approaches is given.

## 1 Introduction

Before the first observation of events with large rapidity gaps in deep inelastic scattering at HERA in 1993 [1, 2], diffractive reactions have been studied and were implemented into Monte Carlo programs:

The POMPYT [3] Monte Carlo program is based on the Ingelman-Schlein ansatz [4] assuming a partonic structure of the pomeron  $P$  and is suitable for a description of the full hadronic final state in diffractive  $e - p$  scattering.

The DIFFVM [5] Monte Carlo program describes elastic vector-meson production assuming the vector meson dominance model with a parameterization of the vector-meson proton scattering cross section based on hadron hadron scattering.

The EPJPSI [6, 7] program, a Monte Carlo for inelastic  $J/\psi$  production also included a simple model for elastic  $J/\psi$  production together with a simulation of inelastic diffractive  $J/\psi$  production, both based on the Ingelman-Schlein ansatz [4].

---

<sup>1</sup> To appear in *Proc. of the LISHEP workshop on diffractive physics*, edited by A. Santoro (Rio de Janeiro, Brazil, Feb 16 - 20, 1998)

Shortly after the observation of large rapidity gap events at HERA, the RAPGAP [8, 9] Monte Carlo program, and a improved version of the POMPYT [10, 11, 12] Monte Carlo program became available. Like POMPYT, RAPGAP was originally based on the Ingelman-Schlein ansatz [4] and suitable for a description of the full hadronic final state in diffractive  $e - p$  scattering. With the same ansatz, diffractive final states were later also included in the Monte Carlo program ARIADNE [13, 14].

In 1995 a new approach to describe events with large rapidity gaps was proposed by Edin, Ingelman and Rathsman [15, 16, 17, 18, 19] and Buchmüller and Hebecker [20, 21, 22, 23, 24]. Independently both groups attempted to explain the production of large rapidity gap events by interactions of the colored partons from the hard interaction process with the color field of the proton. This interaction was described by the so-called soft color interactions (SCI) [15, 16, 17, 18, 19] or within a semi - classical approach [20, 21, 22, 23, 24], respectively.

In the meantime substantial progress in the theoretical understanding of diffraction has been made, which enabled a subset of diffractive scattering to be described in terms of perturbative QCD: Vector meson production (see for example [25, 26]) and the production of exclusive high  $p_T$  jets [27, 28, 29, 30, 31, 32] and charm [33, 34] (for a more complete list of references and a summary see [35]). The perturbative QCD approach for high  $p_T$  exclusive di-jet processes and heavy quark production has been implemented in the RAPGAP [9] Monte Carlo. Vector-meson production calculated in perturbative QCD is implemented in the Monte Carlos DIPSI [36], RHODI [37] and HITVM [38].

In a completely different approach the pomeron  $IP$  is assumed to have direct couplings to quarks. This has been calculated and implemented in the Monte Carlo program VBLY [39].

In the following I shall concentrate on the two Monte Carlo programs RAPGAP 2.06 [9] and LEPTO 6.5 [16]. RAPGAP is discussed as a representative of multi - purpose Monte Carlo programs including a description of the resolved pomeron model according to the Ingelman-Schlein ansatz and the pQCD description for diffractive  $q\bar{q}$  production. Both the resolved pomeron model and the perturbative QCD description are successfully describing present data on hadronic energy flow and particle spectra as well as high  $Q^2$  production of  $J/\psi$  mesons. LEPTO is the only alternative model attempting to describe rapidity gap events with the soft color interaction approach, without involving the concept of a Pomeron. A comparison of the different approaches (resolved pomeron, pQCD and SCI) is made for a few experimental observables.

## 2 Kinematics and the total cross section

In a diffractive process  $e + p \rightarrow e' + p' + X$  where  $p'$  represents the elastically scattered proton or a low mass final state, and  $X$  stands for the diffractive

hadronic state, the cross section can be written as [40]:

$$\frac{d^4\sigma(ep \rightarrow e'Xp')}{dy dQ^2 dx_{\mathbb{P}} dt} = \frac{4\pi\alpha^2}{yQ^4} \left( \left(1 - y + \frac{y^2}{2}\right) F_2^{D(4)}(x, Q^2; x_{\mathbb{P}}, t) - \frac{y^2}{2} F_L^{D(4)}(x, Q^2; x_{\mathbb{P}}, t) \right) \quad (1)$$

with  $y = (q.p)/(e.p)$ ,  $Q^2 = -q^2 = (e - e')^2$ ,  $x_{\mathbb{P}} = (q.P)/(q.p)$  and  $t = (p - p')^2$  where  $e$  ( $e'$ ) are the four vectors of the incoming (scattered) electron, the Bjorken  $x$  variable  $x = Q^2/(y \cdot s)$  with the total center of mass energy  $s = (e+p)^2$ ,  $p$  ( $p'$ ) are the four vectors of the incoming (scattered) proton,  $q = e - e'$  is the four vector of the exchanged photon and  $\mathbb{P} = p - p'$  corresponds to the four vector of the pomeron. In analogy to Bjorken- $x$ , one can define  $\beta = x/x_{\mathbb{P}}$ . In terms of experimental accessible quantities, these variables can be expressed as:

$$x_{\mathbb{P}} = \frac{Q^2 + M_X^2}{Q^2 + W^2} \quad (2)$$

$$\beta = \frac{Q^2}{Q^2 + M_X^2} \quad (3)$$

with  $M_X$  being the invariant mass of the diffractive ( $\gamma^*\mathbb{P}$ ) system and  $W$  the mass of the  $\gamma^*p$  system. Independently of the underlying picture of diffraction  $x_{\mathbb{P}}$  and  $\beta$  can be defined. However the inclusive structure function  $F_2^{D(4)}$  or equivalently the  $\gamma^*p$  cross section provides no direct information concerning the hadronic final state. In order to construct a Monte Carlo describing the hadronic final state, the structure function  $F_2^D$  has to be interpreted in terms of partonic subprocesses:

- **Resolved pomeron a la Ingelman and Schlein**

In the Ingelman-Schlein model [4]  $F_2^{D(4)}$  can be written as the product of the probability of finding a pomeron,  $f_{p\mathbb{P}}$ , in the proton and the structure function  $F_2^{\mathbb{P}}$  of the pomeron:

$$F_2^{D(4)}(\beta, Q^2; x_{\mathbb{P}}, t) = f_{p\mathbb{P}}(x_{\mathbb{P}}, t) F_2^{\mathbb{P}}(\beta, Q^2) \quad (4)$$

In analogy to the quark - parton - model of the proton,  $\beta$  can be interpreted as the momentum fraction of the total pomeron momentum carried by the struck quark and  $F_2^{\mathbb{P}}(\beta, Q^2)$  can be described in terms of momentum weighted quark density functions in the pomeron.

- **pQCD calculation of diffraction**

The pQCD calculation of diffraction is applicable mainly to exclusive high  $p_T$  di-jet production, but in the model of [27] estimates on the total inclusive diffractive cross section are given. The calculation of diffractive di-jet production can be performed using pQCD for large photon virtualities  $Q^2$  and high  $p_T$  of the  $q(\bar{q})$  jets [27, 28, 29, 30, 31, 32] or for heavy quarks [33, 34].

The process is mediated by two gluon exchange. Different assumptions on the nature of the exchanged gluons can be made: in [28, 29] the gluons are non perturbative, in [27] they are a hybrid of non perturbative and perturbative ones and in [30, 31] they are taken from a NLO parameterization of the proton structure function [41, 42]. The cross section is essentially proportional to the gluon density squared of the proton:  $\sigma \sim [x_{\mathcal{P}} G_p(x_{\mathcal{P}}, \mu^2)]^2$  with the scale  $\mu^2 = p_T^2/(1 - \beta)$ . In the case of heavy quarks the cross section is finite for all  $p_T$ , and the scale is taken to be  $\mu^2 = (p_T^2 + m_f^2)/(1 - \beta)$  [33, 34], with  $m_f$  being the mass of the heavy quark.

Due to the different gluon density parameterizations, different  $x_{\mathcal{P}}$  dependencies of the cross sections are expected and further discussed in [30, 31], where also numerical estimates are presented.

- **Semi-classical approach of Buchmüller, McDermott and Hebecker**

Buchmüller et al. [20, 21, 22, 23, 24] attempt to describe  $\gamma^* + p \rightarrow q + \bar{q} + p'$  and  $\gamma^* + p \rightarrow q + \bar{q} + g + p'$  in a semi - classical approach where the partons of the hard scattering subprocess interact with the color field of the proton. The cross section of the first process turns out to be of similar structure as in the pQCD calculation of [31] and is proportional to a constant, which can be interpreted in the semi-classical approach as the proton gluon density squared. The  $q\bar{q}g$  process is described with a usual boson gluon fusion subprocess, but involving an effective diffractive gluon density [23]:

$$x_{\mathcal{P}} g^D(x_{\mathcal{P}}, \beta) = \frac{C_1}{\beta \cdot C_g - \beta + 1} \cdot \frac{1}{x_{\mathcal{P}}} \quad (5)$$

with  $C_1$  and  $C_g$  being free parameters. Note that with  $C_g = 1$  the gluon density only depends on  $x_{\mathcal{P}}$ . Moreover in this approach only a  $1/x_{\mathcal{P}}$  dependence appears, in contrast to other models, where a  $1/x_{\mathcal{P}}^{1+\epsilon}$  is present. In order to account for non-zero  $t$  the dipole form factor of the proton is applied.

- **Soft Color Interaction (SCI)**

In this approach events with large rapidity gaps are produced by soft color interactions that change the color charge of the partons originating from the hard interaction process [15, 16, 17, 18, 19], before fragmentation. No pomeron is explicitly introduced. All parameters in this model are determined by non-diffractive deep inelastic scattering, except the probability for a soft color interaction  $R_{SCI}$ .

### 3 The partonic final state

In this section I shall first describe the procedure to obtain a model of the hadronic final state in diffraction using diffractive parton densities, which I shall call the *resolved pomeron* model. Here it is not necessary to assume factorization as in the Ingelman-Schlein ansatz. Then I shall describe the MC implementation of the perturbative QCD approach and in which way it differs from the resolved pomeron model. At the end I shall discuss the soft color interaction (SCI) model.

#### 3.1 The partonic final state in the resolved pomeron model

In close analogy to inclusive  $e - p$  scattering, where  $F_2(x, Q^2)$  is given by  $F_2(x, Q^2) = \sum_i e_i^2 \cdot x q_i(x, Q^2)$  with  $e_i^2$  being the electric charge and  $q_i(x, Q^2)$  the parton density function of quark  $i$ , diffractive parton densities can be defined such, that the sum over  $x_{\mathcal{P}} \cdot q_i^D(\beta, Q^2; x_{\mathcal{P}}, t)$  gives  $F_2^{D(4)}$ . With such a definition the hadronic final state in diffractive processes can be constructed similarly to that of non diffractive scattering, by the 0th order  $\alpha_s$  process  $\gamma^* q \rightarrow q'$  (QPM) and the 1st order  $\alpha_s$  processes  $\gamma^* q \rightarrow qg$  (QCDC) and  $\gamma^* g \rightarrow q\bar{q}$  (BGF). In this procedure the incoming parton (a quark or a gluon) has zero transverse momentum (except from a possible small intrinsic  $k_T$ ), leaving a remnant behind, which does not take part in the hard interaction and therefore also has zero (or small)  $k_T$ . This is in contrast to the pQCD calculation of [27, 28, 29, 30, 31, 32] for  $\gamma^* p \rightarrow q\bar{q}p'$ , where both quark and anti-quark participate in the hard interaction and therefore have finite  $k_T$ , without leaving a remnant behind.

With the knowledge of  $x_{\mathcal{P}} \cdot q_i^D(\beta, Q^2; x_{\mathcal{P}}, t)$  and  $x_{\mathcal{P}} \cdot g_i^D(\beta, Q^2; x_{\mathcal{P}}, t)$  the total cross section can be described in terms of scattering off a virtual photon on a quark or anti-quark. However this quark may have been originated from another parton, producing a different hadronic final state. The process where an initial parton carrying a momentum fraction  $x_i$ , splits into other partons which then undergo hard scattering with the photon, can be simulated in QCD parton showers based on the leading log DGLAP [43, 44, 45, 46] splitting functions in leading order  $\alpha_s$ .

A more detailed simulation of leading order  $\alpha_s$  processes like  $\gamma^* g \rightarrow q\bar{q}$  (BGF, Fig. 1b.) and  $\gamma^* q \rightarrow qg$  (QCD - Compton, Fig. 1c.) is obtained when the exact  $O(\alpha_s)$  QCD matrix elements for these processes are included.

The decision whether to generate a QPM or a 1st order  $\alpha_s$  event, is based on their relative cross sections at a given  $x$  and  $Q^2$ . Technically for each event the cross section for BGF light quarks, BGF heavy quarks and QCD - Compton

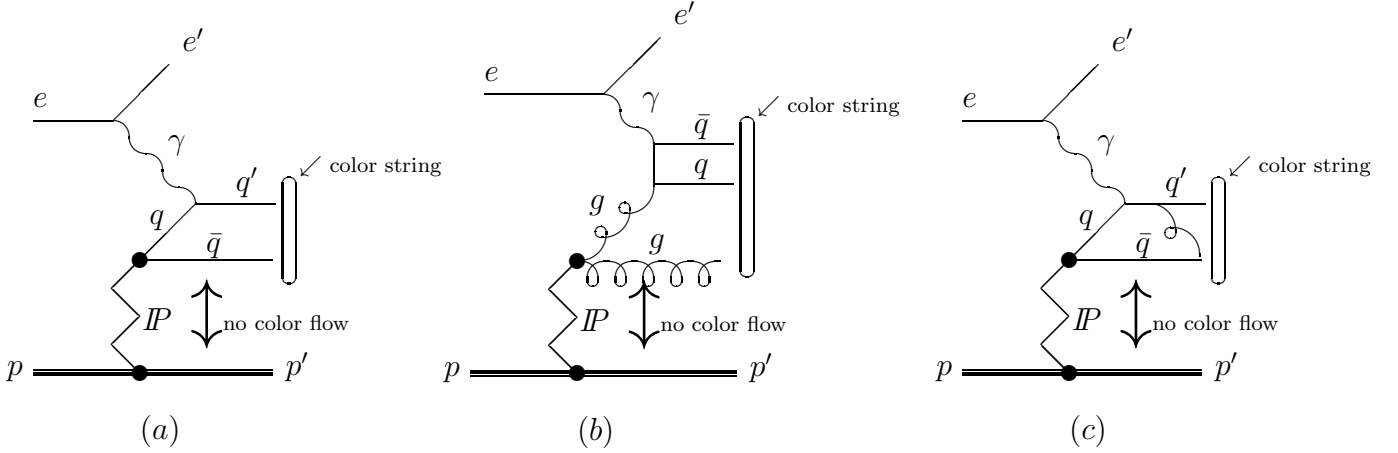


Figure 1: Basic processes for inelastic diffractive lepton nucleon scattering. Indicated are the color strings and the pomeron remnant. *a.* shows the QPM process (0th order  $\alpha_s$ ) for quark scattering. *b.* shows the  $O(\alpha_{em}\alpha_s)$  for photon gluon fusion (the crossed diagram is not shown). The pomeron remnant is a color octet gluon. In *c.* the  $O(\alpha_{em}\alpha_s)$  QCD Compton process (the crossed diagram is not shown) is shown. The pomeron remnant is the same as in *a.*

has to be obtained from a numerical integration including the proper parton densities. If the scale chosen for  $\alpha_s$  and the parton densities is either  $Q^2$  or the invariant mass squared of the two hard partons,  $\hat{s}$ , then the matrix elements can be integrated analytically over one degree of freedom leaving only a one dimensional numerical integration to be done. If, however, the scale is  $p_T^2$  (or any function of it) then  $\alpha_s$  and the parton densities cannot be factorized, and a time consuming two dimensional numerical integration has to be performed. As an alternative the QCD probabilities can be calculated once and stored in a grid. This approach is faster but less accurate. Both options for obtaining the  $O(\alpha_s)$  QCD probabilities are implemented in RAPGAP and LEPTO, where for the latter only the scale  $Q^2$  is implemented.

In order to avoid divergences in the matrix elements for massless quarks a cutoff in  $p_T^{cut}$  (or in other variables like  $\hat{s}$  and  $z$  or  $\hat{t}$ ) has to be specified. The minimum  $p_T^{cut}$  is at least restricted by the requirement that the sum of the order  $\alpha_s$  processes has to be smaller or equal to the total cross section given by  $F_2$  (or  $F_2^{D(4)}$ ). Note that if a too small  $p_T^{cut}$  is used, the prediction from the 1st order  $\alpha_s$  matrix elements might be unreliable since  $\alpha_s$  might be too large to justify the use of pQCD.

Having thus constructed the hard scattering subprocess up to order  $\alpha_s$ , higher order corrections may be simulated by initial and final state parton showers. Because of the strong ordering of virtualities in a DGLAP evolution, the virtuality in the parton showers is restricted by the cutoff  $p_T^{cut}$  for the  $O(\alpha_s)$

matrix elements, since partons having larger  $p_T > p_T^{cut}$  are already generated by the matrix element processes.

This ends the construction of the hard partonic final state, leaving the construction of the final state proton or proton dissociation to be done. The hadronic final state is then constructed by handing the partons over to a fragmentation program like JETSET [47, 48, 49].

### 3.2 Perturbative QCD approach to diffraction

The cross section for  $ep \rightarrow e'q\bar{q}p$  has been calculated in [27, 28, 29, 30, 31, 32]. For the production of light quarks a  $p_T^{cut}$  has to be applied, to regulate the collinear divergence of the matrix element. In the case of heavy quark production [33, 34] the cross section is finite even for small  $p_T$  because of the heavy quark mass.

Since both the quark and the anti-quark participate in the hard interaction, they both receive the same transverse momentum in the  $\gamma^*IP$  system, without producing a remnant, and both final state partons are allowed to further radiate partons in the final state parton shower. This has to be contrasted to the resolved pomeron model, where also a  $q\bar{q}$  final state appears in a QPM process, but there the quarks have vanishing transverse momentum (except from a small intrinsic  $p_T$ ) in the  $\gamma^*IP$  center of mass system and a pomeron remnant is present. Another striking feature of the exclusive  $q\bar{q}$  production in pQCD is a very special azimuthal asymmetry between jet and the lepton plane in the  $\gamma^*IP$  CMS.

These processes have been implemented in RAPGAP, allowing different parameterizations of the gluon density of the proton to be used.

### 3.3 Soft color interaction

A detailed description of the soft color interaction model can be found in [15, 16, 17, 18, 19]. Here only the main characteristics are presented.

In non - diffractive scattering at small  $x$  the most important process is boson - gluon fusion ( $\gamma^*g \rightarrow q\bar{q}$ ). After the hard scattering process and the initial and final state QCD radiation took place, the partons of the hard scattering process travel through the color field of the proton and there is a certain probability for soft color interactions, which can change the color structure without changing the kinematics of the process. The probability for soft color interactions  $R_{SCI}$  is the only free parameter in this model, where  $R_{SCI}$  may be seen as a value of the strong coupling constant  $\frac{\alpha_s}{\pi} \sim 0.2$  at a scale of 0.5 GeV, which is representative for the region below the perturbative cutoff. Large rapidity

gap events can be produced since it can happen that the hard scattering sub-process becomes disconnected in color space from partons of the QCD cascade and the proton remnant. For large rapidity gap events a  $\sim 1/M_X^2$  distribution is generated from the  $\sim 1/\hat{s}$  dependence of the BGF process. Also the  $t$  distribution follows in general an exponential form, determined by the Gaussian width of the distribution of the intrinsic transverse momentum of the partons in the proton (for details see [15, 16, 17, 18, 19]).

The SCI model allows a smooth transition between non-diffractive to diffractive scattering, including also a simulation of Reggeon and  $\pi$  exchange processes, without introducing these exchanges explicitly.

## 4 A simple model for proton dissociation

In this section a simple model for proton dissociation implemented in RAPGAP and based on ideas from PYTHIA [49] is described. When a proton dissociates, it can split into a quark  $q_p$  and di-quark  $di - q_p$  system. The pomeron is assumed to couple to a single quark  $q_p$  only, and therefore the outgoing quark  $q'_p$  carries all of the momentum transfer  $t$  resulting in a finite transverse momentum. The quark to which the pomeron couples carries a momentum fraction  $\chi$  of the protons initial momentum. The momenta of the initial quark  $q_p$  and the di-quark  $di - q_p$  are:

$$q_p \simeq \chi p \tag{6}$$

$$di - q_p \simeq (1 - \chi)p \tag{7}$$

$$q'_p = q_p - IP \simeq \chi p - P \tag{8}$$

where  $\chi = \frac{q \cdot q_p}{q \cdot p}$  with  $q$  ( $q_p$ ,  $p$  and  $IP$ ) being the photon (quark, proton and pomeron) momentum, respectively. In addition the quark and di-quark can receive a primordial  $p_\perp$  according to a Gaussian distribution.

The momentum fraction  $\chi$  can be estimated within the resolved pomeron model:

$$\chi = \frac{x_P}{\beta'} \tag{9}$$

with  $\beta' = \frac{q \cdot IP}{q \cdot q_p}$  being the fraction of the pomeron momentum carried by the quark  $q_p$  and  $x_P = \frac{q \cdot P}{q \cdot p}$ .  $\beta'$  is defined similarly to  $\beta$ , which is used in the structure function  $F_2^{IP}$ . The value of  $x_P$  is already known from the interaction  $\gamma IP$  and  $\beta'$  can be generated according to the quark density of the pomeron.

Instead of using explicitly the parameterization of parton densities in the pomeron, which have been obtained from  $F_2^D$ , a more simple ansatz is chosen, since the scale, at which proton dissociation happens is too small (typically of

the order of  $|t| \ll 1 \text{ GeV}^2$ ) to be used in parton density function parameterizations. For  $\beta'$  different, alternative probability functions  $P_i$  are available:

$$P_1(\beta') = 2(1 - \beta') \quad (10)$$

$$P_2(\beta') = (a + 1)(1 - \beta')^a \quad (11)$$

$$P_3(\beta') = \frac{N}{\beta' \left(1 - \frac{1}{\beta'} - \frac{c}{(1-\beta')}\right)^2} \quad (12)$$

with  $a$  chosen such that  $\langle \beta' \rangle = 1/(a + 2)$  and  $c$  determined by the ratio of masses of the remnant quark and di-quark system. The first option corresponds to a hard quark density of the pomeron. These parameterizations are actually used as the probability functions even in non-diffractive scattering and have been taken from LEPTO [50].

## 5 Vector-meson production

In RAPGAP vector meson production is naturally included in diffractive scattering. This is easiest seen for  $J/\psi$  production. Suppose we have a system of a  $c\bar{c}$  quark pair, plus possibly additional gluons in the final state. If the invariant mass  $4 \cdot m_c^2 < m_x^2 = (q + p_P)^2 < 4 \cdot m_{D^0}^2$  then only  $J/\psi$ 's can be produced ( $\eta_c$  production is not possible because of spin constraints). Technically vector-mesons are produced in the fragmentation program JETSET [47, 48, 49], with the additional restriction that only spin 1 mesons are generated. However there is an uncertainty in the normalization of the cross section, depending on the actual value of  $m_c$  used. The production of the light vector-mesons  $\rho$ ,  $\omega$  and  $\phi$  proceeds in a similar way to that of the  $J/\psi$ , with the ratio  $\rho : \omega = 9 : 1$  being fixed and  $\phi$  vector mesons being only produced from  $s$  quarks.

Exclusive vector meson production implies certain restrictions on the kinematic variables  $x_P$  and  $\beta$ :

$$x_P = \frac{q \cdot p_P}{q \cdot P} = \frac{Q^2 + M_X^2}{Q^2 + W^2} \quad (13)$$

$$\beta = \frac{Q^2}{2 \cdot q \cdot p_P} = \frac{Q^2}{Q^2 + M_X^2} \quad (14)$$

Thus for  $M_X = m_{VM}$  and fixed  $W$  the variables  $x_P$  and  $\beta$  depend only on  $Q^2$ . Thus varying  $Q^2$  implies varying  $x_P$  and  $\beta$ . The effective  $Q^2$  dependence of the  $\gamma^* p \rightarrow VMp$  cross section is stronger ( $\simeq 1/Q^4$ ), than expected from  $\gamma^* p \rightarrow X$  ( $\simeq 1/Q^2$ ).

## 6 Model Comparisons

In this section I shall compare the different approaches to describe diffraction and compare them with data, where available.

## 6.1 Inclusive structure function $F_2^D$

In Fig. 2 the prediction for the diffractive structure function  $F_2^{D(3)}$  of the SCI model (using  $R_{SCI} = 0.5$ ) as implemented in LEPTO 6.5 [16] is compared to the measurement of H1 [51]. It is remarkable that this model, with essentially only one free parameter,  $R_{SCI}$  is able to describe the general trend of the data. However in the low  $Q^2$  and low  $\beta$  region this model overshoots the data. For comparison the results from the resolved pomeron model are also shown in Fig. 2. The fact that this model describes the data is not surprising, since the  $Q^2$  evolved parton densities obtained from a fit to  $F_2^{D(3)}$  [51] are used.

The total cross section of the perturbative QCD approach is not shown, since it depends on the  $p_T$  cutoff needed for the light quark contribution.

## 6.2 Proton Dissociation

Experimentally proton dissociation can be studied, when the system  $M_X$ , associated with the  $\gamma$  vertex, and the system  $M_Y$ , associated with the proton vertex, can be separated. This can be achieved by searching for the largest rapidity gap in an event following the procedure of [51]. The mass distribution  $M_Y$  of the  $p$  - dissociative system in  $e - p$  diffractive events obtained from the RAPGAP Monte Carlo is shown in Fig. 3a. The difference between the different options for  $P(\beta')$  is shown. In Fig. 3b. a comparison between RAPGAP and LEPTO is shown. At small masses  $M_Y$  ( $M_Y < 10$  GeV) a  $\sim 1/M_Y$  spectrum is obtained both for RAPGAP and LEPTO and only at larger masses  $M_Y > 10$  GeV (not shown in Fig. 3) a typical  $\sim 1/M_Y^2$  dependence is observed. Even with proton dissociation switched on, a proton will emerge after fragmentation when the momentum transfer is small and the mass of the  $q - di - q$  system remains below the threshold for multi-particle production.

The SCI model automatically also simulates proton dissociation since the color flow between the hard scattering and the proton remnant can be broken anywhere in rapidity. In Fig. 3 the  $M_Y$  spectrum obtained from LEPTO 6.5 is shown. Also in the SCI model a general  $\sim 1/M_Y$  spectrum is obtained, however the ratio of proton - elastic to proton dissociative events is different to that obtained from RAPGAP.

## 6.3 Hadronic energy flow

In Fig. 4 the energyflow in diffractive scattering predicted by the various models is compared to the measurement of H1 [52]. The prediction of the SCI model (dashed line in Fig. 4) is very close to the prediction of the resolved pomeron model in RAPGAP (solid line), and both give a good description of the data.

The SCI model is rather successful in describing properties of the hadronic final state in diffraction without involving the concept of a pomeron.

Also shown in Fig. 4 is the energy flow predicted from the perturbative QCD calculation (dotted line) as implemented in RAPGAP. The gluon density was taken from the GRV HO parameterization and  $p_T > 1$  GeV was required for the final state quarks. Both final state quarks were allowed to emit further QCD radiation. There is a remarkable agreement between this prediction and the data, considering that it has no free parameter left. In the lowest  $M_X$  bin at central rapidities ( $\eta^* \sim 0$ ) a small dip is observed, which is understood as a consequence of the finite  $p_T$  cutoff for the final state quarks. One has to note that no free parameter is left in this calculation. It is a great success that the energy flow can be understood in terms of perturbative QCD.

From the comparison of the different approaches to describe diffraction with data on the hadronic energy flow, no final conclusion on the underlying physics process can yet be made. All the very different approaches describe the available data reasonably well. Different and more sensitive measurements are obviously needed to differentiate between the various approaches.

## 6.4 $\phi$ asymmetries of jets and heavy quarks

The very specific signature of the perturbative QCD calculation becomes apparent only, when more detailed final state properties are considered. One of the main differences of the perturbative QCD calculation to both the resolved pomeron model and as well as to the SCI model is the absence of a pomeron remnant. This a signature can be investigated with exclusive high  $p_T$  di - jet events. In that case the invariant mass of the jet - jet system  $\hat{s}_{jj}$  is identical to the total invariant mass of the diffractive system  $M_X^2$ . However depending on the jet algorithm used to identify the high  $p_T$  jets, a certain fraction of hadronic energy might not be associated to the jets, which might cause a problem for the identification of exclusive di - jet events.

For a study of the effects of different jet algorithms, the following kinematic cuts are applied:  $0.1 < y < 0.7$ ,  $5 < Q^2 < 80$  GeV<sup>2</sup>  $x_P < 0.05$  and  $p_T^{jet} > 2$  GeV. Using the  $k_T$  jet algorithm [53, 54, 55] with a  $y_{cut}$  such that two hard jets with  $k_T > 2$  GeV and a possible remnant jet are reconstructed in the Breit frame (labeled invariant  $k_t$ ), a distribution of  $R_{jj} = \hat{s}_{jj}/M_X^2$  is obtained, as shown in Fig. 5 with the solid line histogram. For an ideal jet reconstruction  $R_{jj} = 1$  is expected. However one sees large effects due to the jet reconstruction. The results using different jet algorithms like cone type jet algorithm [56] or the inclusive  $k_T$  algorithm [53, 54, 55] are also shown in Fig. 5. For comparison also the distribution obtained from a BGF type process in the resolved pomeron model is shown. Exclusive di - jet events are best identified using the invariant  $k_t$  algorithm.

The most striking feature of the perturbative QCD calculation of diffractive  $q\bar{q}$  final state is the  $\phi$  asymmetry between the lepton and the quark plane in the  $\gamma^*p$  center of mass system. It is difficult to identify the quark - jet at hadron level, therefore the jet with the largest  $p_T$  is used. The azimuthal asymmetry of the two gluon exchange mechanism obtained after jet reconstruction is shown in Fig. 6, where also a comparison with the azimuthal asymmetry expected from a diffractive BGF process with one gluon exchange (from a resolved pomeron) is given. Even at the hadron level the difference between the two approaches is clearly visible.

However one has to be careful using this pQCD description of high  $p_T$  dijet production, since it is expected to be dominant only in a region where  $Q^2 \gg p_T^2$ . In other regions of phase space where  $Q^2 \sim p_T^2$  the contribution from  $q\bar{q}g$  final states are expected to become dominant. Such a calculation is just being performed [57].

As the calculation of a diffractive  $q\bar{q}$  state can also be extended to heavy quark production [33, 34], the difficulty of identifying high  $p_T$  di-jets may be avoided by the observation of  $D^*$  mesons. In Fig. 7a the  $\phi$  asymmetry is shown for  $D^*$  mesons produced by the two gluon exchange mechanism and compared to the prediction from a BGF process in the resolved pomeron picture, where the kinematic region is specified by:  $0.06 < y < 0.6$ ,  $2 < Q^2 < 100 \text{ GeV}^2$ ,  $x_P < 0.05$ ,  $p_T^{D^*} > 1 \text{ GeV}$  and  $|\eta^{D^*}| < 1.25$ . This process may thus also be used to differentiate between the two approaches. One should note that the different  $\phi$  distribution observed here, as compared to ones from the jets, is due to the cuts in the laboratory system used by the experiments to identify the  $D^*$  meson. Without the  $p_T^{D^*}$  cut, the  $\phi$  distribution looks the same as for the jets. In Fig. 7b the  $\phi$  asymmetry at parton level without the acceptance cuts is shown.

## 6.5 Vector-meson production

The cross section for vector meson production depends crucially on the underlying subprocess. For the calculation the charm mass was set to  $m_c = 1.5 \text{ GeV}$ . First I shall describe  $J/\psi$  production using a recent parameterization of  $F_2^{D(3)}(x_P, \beta, Q^2)$  of the H1 collaboration [51]. This parameterization is based on a significant diffractive gluon density. Within the model described before and implemented in RAPGAP,  $J/\psi$  production at large  $Q^2$  as measured by H1 [58] and ZEUS [59] can be well described, both as a function of  $Q^2$  and  $W$  (Fig. 8, solid line). It is remarkable that a  $\sim 1/Q^4$  dependence of the photon proton cross section appears consistent with the data, which is usually interpreted as a higher twist effect. Using diffractive parton densities, this  $Q^2$  dependence follows naturally from the  $\beta$  dependence of the structure function  $F_2^{D(3)}$ , since as shown before, changing  $Q^2$  is equivalent with changing  $\beta$  for a fixed mass of the vector-meson.

In the perturbative QCD approach heavy quarks can be produced and, as mentioned before, the cross section is essentially proportional to the gluon density squared. For heavy quarks no restriction on the  $p_T$  of the quarks is necessary, and therefore the model of vector meson production described above can be applied. In Fig. 8 the prediction from this calculation using the GRV HO parameterization of the gluon density in the proton is shown with the dashed line. The cross section agrees rather well with the data, both in shape and normalization. The calculation agrees well with the data and also with the approach using a parameterization of diffractive parton densities. However one should keep in mind that the diffractive gluon density obtained from scaling violations of  $F_2^{D(3)}$  is only poorly constrained, so that there is still a significant normalization uncertainty.

A smaller value for the charm quark mass gives a larger phase space and a larger cross section in addition to a change in the scale for  $\alpha_s$  and for the parton distribution functions which is essentially set by the charm quark mass. Different choices of the charm mass result in an uncertainty in the overall normalization, which has been estimated:  $\sigma_{J/\psi}^{m_c=1.5} / \sigma_{J/\psi}^{m_c=1.35} \simeq 0.6$ . A similar uncertainty in normalization is also found for the color singlet model of inelastic charm production, including the non relativistic wave function of the  $J/\psi$  - meson [60].

Given these uncertainties, both approaches are in fair agreement. If transverse and longitudinally produced vector meson can be separated, differences between the two approaches should show up, since in the perturbative calculation the longitudinal part becomes large at large  $Q^2$ , which is not expected in the resolved pomeron approach.

One should note that the energy dependence of the cross section in the perturbative approach emerges naturally from the gluon density in the proton, whereas using a parameterization of diffractive parton densities, the  $x_{\mathbb{P}}$  dependence has been inserted by hand to fit  $F_2^{D(3)}$ . However it is a success, that the energy dependence obtained from  $F_2^{D(3)}$  can be used to describe also  $J/\psi$  production.

## 7 Summary

The implementation of very different models for diffraction in deep inelastic scattering has been described. It is found that available data on hadronic final state properties are reasonably well described by the resolved pomeron model using a parameterization of diffractive parton densities, by the soft color interaction model and the perturbative QCD calculation involving two gluon exchange. It is shown that the different models can be distinguished, if differential distributions are considered. One particular example is diffractive

charm production in deep inelastic scattering, where the  $\phi$  dependence of the cross section shows a very different behavior in the two gluon exchange model compared to the resolved pomeron model.

It has been also shown that vector meson production can be nicely described within a simple approach, both using the resolved pomeron model and the pQCD calculation via two gluon exchange.

Model predictions for the proton dissociative system have been presented in two different approaches, within RAPGAP and the soft color interaction approach implemented in LEPTO 6.5. Both models gave similar predictions.

As more precise data on the hadronic final state in deep inelastic diffraction are expected soon, it might be possible to distinguish and separate the various approaches to diffraction and new and interesting insights into the structure of the proton are expected.

## Acknowledgements

It was a great pleasure to participate at this interesting workshop. I am grateful to the organizers A. Santoro and A. Brandt for this lively workshop and the stimulating atmosphere. I am grateful to M. Erdmann, J. Gayler, G. Ingelman and L. Jönsson for careful reading of the manuscript.

## References

- [1] ZEUS Collaboration; M. Derrick et al., Phys. Lett. **B 315**, 481 (1993).
- [2] H1 Collaboration; T. Ahmed et al., Nucl. Phys. **B 429**, 477 (1994).
- [3] P. Bruni, G. Ingelman, and A. Solano, in *Proc. of the Workshop on Physics at HERA, Vol. 1*, edited by W. Buchmüller and G. Ingelman (DESY, Hamburg, 1991), Vol. 311, p. 363.
- [4] G. Ingelman and P. Schlein, Phys. Lett. **B 152**, 256 (1985).
- [5] B. List, Diploma thesis, Techn. Univ. Berlin, H1 note: H1-10/93-319 (unpublished).
- [6] H. Jung, in *Proc. of the Workshop on Physics at HERA, Vol. 3*, edited by W. Buchmüller and G. Ingelman (DESY, Hamburg, 1991), p. 1488, PITHA 92/10.
- [7] H. Jung, *EPJPSI: A Monte Carlo generator for  $J/\psi$  mesons in high energy  $\gamma - p$ ,  $e - p$  and  $p - \bar{p}$  collisions, version 3.3*, Lund University, 1995, <http://www-h1.desy.de/~jung/epjpsi.html>.

- [8] H. Jung, *Comp. Phys. Comm.* **86**, 147 (1995).
- [9] H. Jung, *The RAPGAP Monte Carlo for Deep Inelastic Scattering, version 2.06*, Lund University, 1998, <http://www-h1.desy.de/~jung/rapgap.html>.
- [10] P. Bruni and G. Ingelman, *Phys. Lett.* **B 311**, 317 (1993).
- [11] P. Bruni and G. Ingelman, in *Proc. of the EPS International High Energy Physics Conference*, edited by J. Carr and M. Perrottet (Editions Frontieres, Marseille, France, 22-28 Jul, 1993), DESY 93-187.
- [12] P. Bruni, A. Edin, and G. Ingelman, *POMPYT version 2.6 - A Monte Carlo to simulate diffractive hard scattering processes*, 1996, <http://www3.tsl.uu.se/the/pompnyt/>.
- [13] L. Lönnblad, *Comp. Phys. Comm.* **71**, 15 (1992).
- [14] L. Lönnblad, *Z. Phys.* **C 65**, 285 (1995), CERN-TH-7307-94.
- [15] A. Edin, G. Ingelman, and J. Rathsman, in *Proc. of the Workshop on Deep Inelastic Scattering and QCD*, edited by J. Laporte and Y. Sirois (Paris, April 24 - 28, 1995).
- [16] G. Ingelman, A. Edin, and J. Rathsman, *Comp. Phys. Comm.* **101**, 108 (1997).
- [17] A. Edin, G. Ingelman, and J. Rathsman, *Phys. Lett.* **B 366**, 371 (1996).
- [18] A. Edin, G. Ingelman, and J. Rathsman, *Z. Phys.* **C 75**, 57 (1997), hep-ph/9605281.
- [19] G. Ingelman, in *Proc. of the LISHEP workshop on diffractive physics*, edited by A. Santoro (Rio de Janeiro, Brazil, Feb 16 - 20, 1998).
- [20] W. Buchmüller and A. Hebecker, in *Proc. of the Workshop on Deep Inelastic Scattering and QCD*, edited by J. Laporte and Y. Sirois (Paris, April 24 - 28, 1995).
- [21] W. Buchmüller and A. Hebecker, *Phys. Lett.* **B 355**, 573 (1995), DESY 95-077.
- [22] W. Buchmüller, M. McDermott, and A. Hebecker, *Nucl. Phys.* **B 487**, 283 (1997), hep-ph/9607290.
- [23] W. Buchmüller, M. McDermott, and A. Hebecker, *Phys. Lett.* **B 410**, 304 (1997), hep-ph/9706354.
- [24] W. Buchmüller, M. McDermott, and A. Hebecker, *Phys. Lett.* **B 404**, 353 (1997), hep-ph/9703314.

- [25] M. Ryskin, *Z. Phys.* **C 57**, 89 (1993).
- [26] S.J. Brodsky et al., *Phys. Rep.* **50**, 3134 (1994).
- [27] M. Wusthoff, Photon diffractive dissociation in deep inelastic scattering, 1995, PhD thesis, DESY-95-166.
- [28] M. Diehl, Diffraction in electron - proton collisions, 1996, PhD thesis.
- [29] M. Diehl, *Z. Phys.* **C 76**, 499 (1997), hep-ph/9610430.
- [30] J. Bartels *et al.*, in *Proc. of the Workshop on Future Physics at HERA*, edited by A. De Roeck, G. Ingelman, and R. Klanner (DESY, Hamburg, 1996), hep-ph/9609239.
- [31] J. Bartels, H. Lotter, and M. Wüsthoff, *Phys. Lett.* **B 379**, 239 (1996), hep-ph/9602363.
- [32] J. Bartels, C. Ewerz, H. Lotter, and M. Wusthoff, *Phys. Lett.* **B 386**, 389 (1996), hep-ph/9605356.
- [33] H. Lotter, *Phys. Lett.* **B 406**, 171 (1997), hep-ph/9612415.
- [34] M. Diehl, *Eur. Phys. J.* **C 1**, 293 (1998), hep-ph/9701252.
- [35] H. Abramowicz, J. Bartels, L. Frankfurt, and H. Jung, in *Proc. of the Workshop on Future Physics at HERA*, edited by A. De Roeck, G. Ingelman, and R. Klanner (DESY, Hamburg, 1996), p. 635.
- [36] M. Arneodo, L. Lamberti, and M. Ryskin, *Comp. Phys. Comm.* **100**, 195 (1997), DESY -96-149 hep-ph/9610286.
- [37] A. Garfagnini, L. Iannotti, and L. Lamberti, RHODI Monte Carlo (unpublished).
- [38] L. West, HITVM Monte Carlo for high  $t$  vectormeson production (unpublished).
- [39] J. Vermaseren, F. Barreiro, L. Labarga, and F. Yndurain, Pomeron and jet events at HERA, 1997, DESY 97-031 and hep-ph/9611444.
- [40] G. Ingelman and K. Prytz, *Z. Phys.* **C58**, 285 (1993).
- [41] M. Glück, E. Reya, and A. Vogt, *Z. Phys.* **C 53**, 127 (1992).
- [42] M. Glück, E. Reya, and A. Vogt, *Phys. Lett.* **B 306**, 391 (1993).
- [43] V. Gribov and L. Lipatov, *Sov. J. Phys.* **15**, 438 and 675 (1972).
- [44] L. Lipatov, *Sov. J. Phys.* **20**, 94 (1975).

- [45] G. Altarelli and G. Parisi, Nucl. Phys. **B 126**, 298 (1977).
- [46] Y. Dokshitzer, Sov. Phys. JETP **46**, 641 (1977).
- [47] T. Sjöstrand, Comp. Phys. Comm. **39**, 347 (1986).
- [48] T. Sjöstrand and M. Bengtsson, Comp. Phys. Comm. **43**, 367 (1987).
- [49] T. Sjöstrand, Comp. Phys. Comm. **82**, 74 (1994).
- [50] G. Ingelman, in *Proc. of the Workshop Physics at HERA (1991) Vol. 3, 1366*, edited by W. Buchmüller and G. Ingelman (DESY, Hamburg, 1991).
- [51] H1 Collaboration; C. Adloff et al., Z. Phys. **C 76**, 613 (1997).
- [52] H1 Coll. C. Adloff et al., Phys. Lett. **B 428**, 206 (1998), DESY 98-029.
- [53] S. Catani, Y. Dokshitzer, and B. Webber, Phys. Lett. **B 285**, 291 (1992).
- [54] S. Ellis and D. Soper, Phys. Rev. **D 48**, 3160 (1993).
- [55] S. Catani, Y. Dokshitzer, M. Seymour, and B. Webber, Nucl. Phys. **B 406**, 187 (1993).
- [56] M. Seymour, Z. Phys. **C 62**, 127 (1994).
- [57] J. Bartels, in *Proc. of the LISHEP workshop on diffractive physics*, edited by A. Santoro (Rio de Janeiro, Brazil, Feb 16 - 20, 1998).
- [58] H1 Collaboration; S. Aid *et al.*, Nucl. Phys. **B 468**, 3 (1996).
- [59] ZEUS Collaboration; J. Breitweg *et al.*, Exclusive vector meson production in deep inelastic scattering at HERA, contributed paper 639 to HEP97 Aug 9 - 26 1997, Jerusalem, 1997.
- [60] M. Kraemer, Inclusive  $J/\psi$  photoproduction at HERA, 1997, hep-ph/9707449.
- [61] H1 Collaboration; S. Aid *et al.*, Elastic Production of  $J/\psi$  mesons in photoproduction and at high  $Q^2$  at HERA, contributed paper 242 to HEP97 Aug 9 - 26 1997, Jerusalem, 1997.

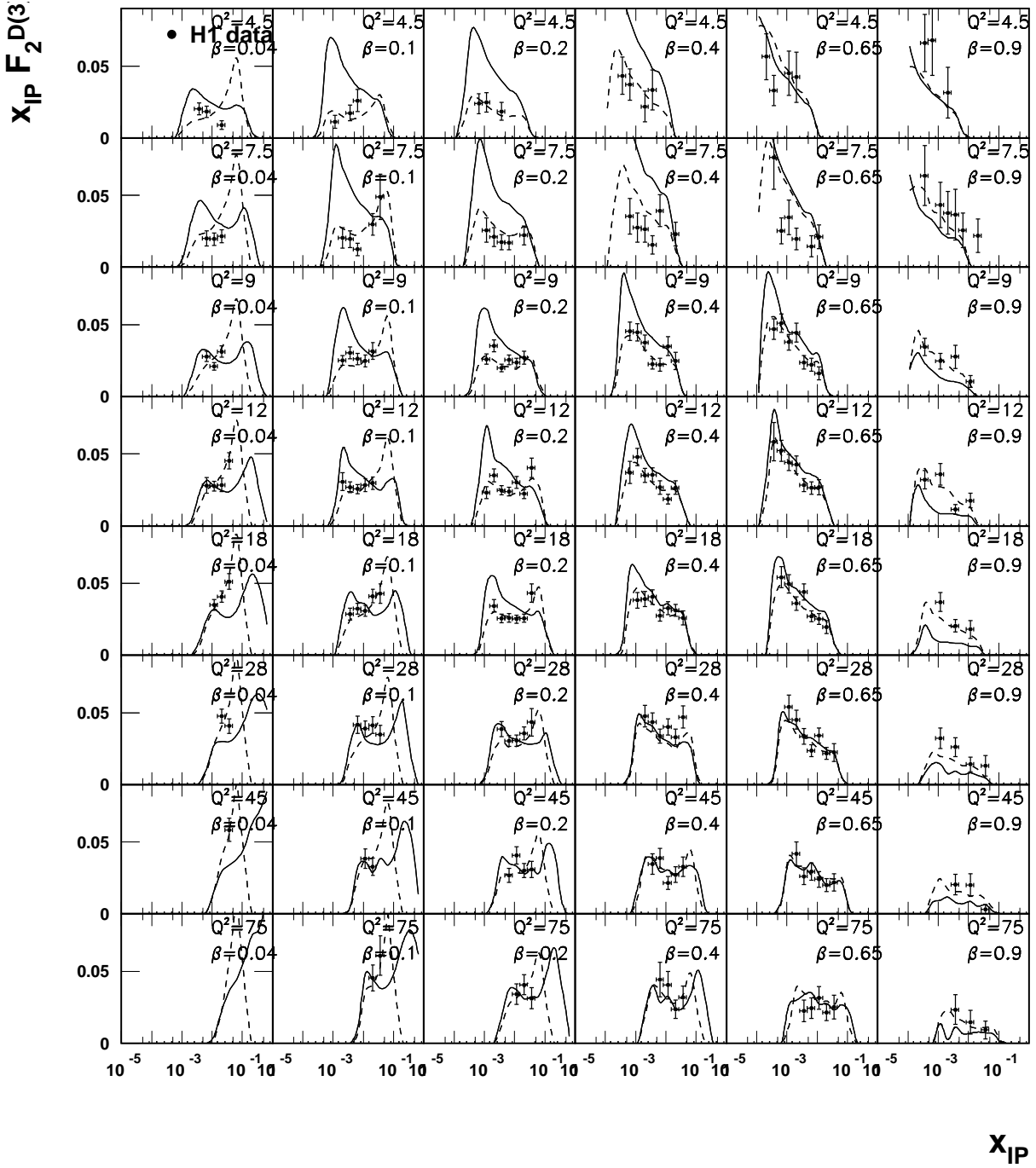


Figure 2: The diffractive structure function  $x_{IP} \cdot F_2^{D(3)}$  [51]. The solid line shows the prediction of the soft color interaction model LEPTO 6.5 with  $R_{SCI} = 0.5$ . For comparison also the result from the resolved pomeron model is shown, using the  $Q^2$  evolved parton densities from a fit to  $F_2^{D(3)}$ .

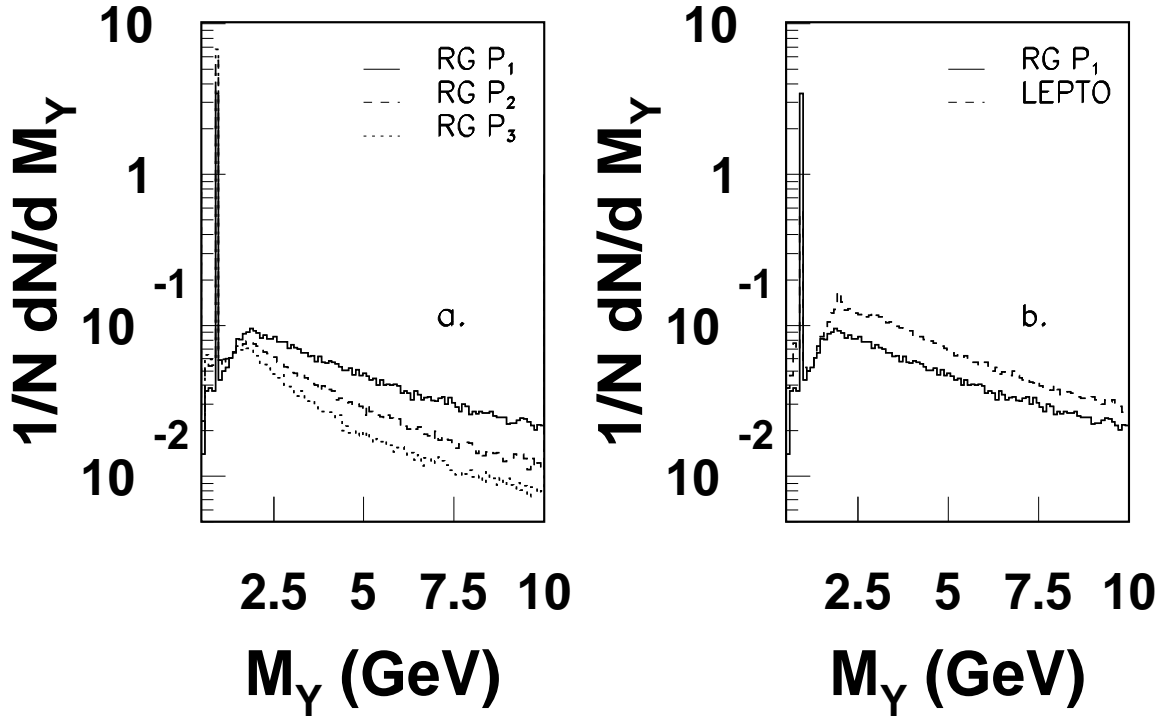


Figure 3: The spectrum  $M_Y$  for  $e - p$  events, with  $x_P < 0.1$  and  $|t| < 1 \text{ GeV}^2$  in the range  $0.01 < y < 0.6$ ,  $5 < Q^2 < 80$ . In *a.* the RAPGAP predictions for different parameterization of the quark splitting functions  $P_i(\beta')$ , as described in the text, are shown. In *b.* the solid line shows the prediction from RAPGAP with  $P_1(\beta')$  and the dashed line shows the prediction from LEPTO 6.5 with  $R_{SCI} = 0.5$ .

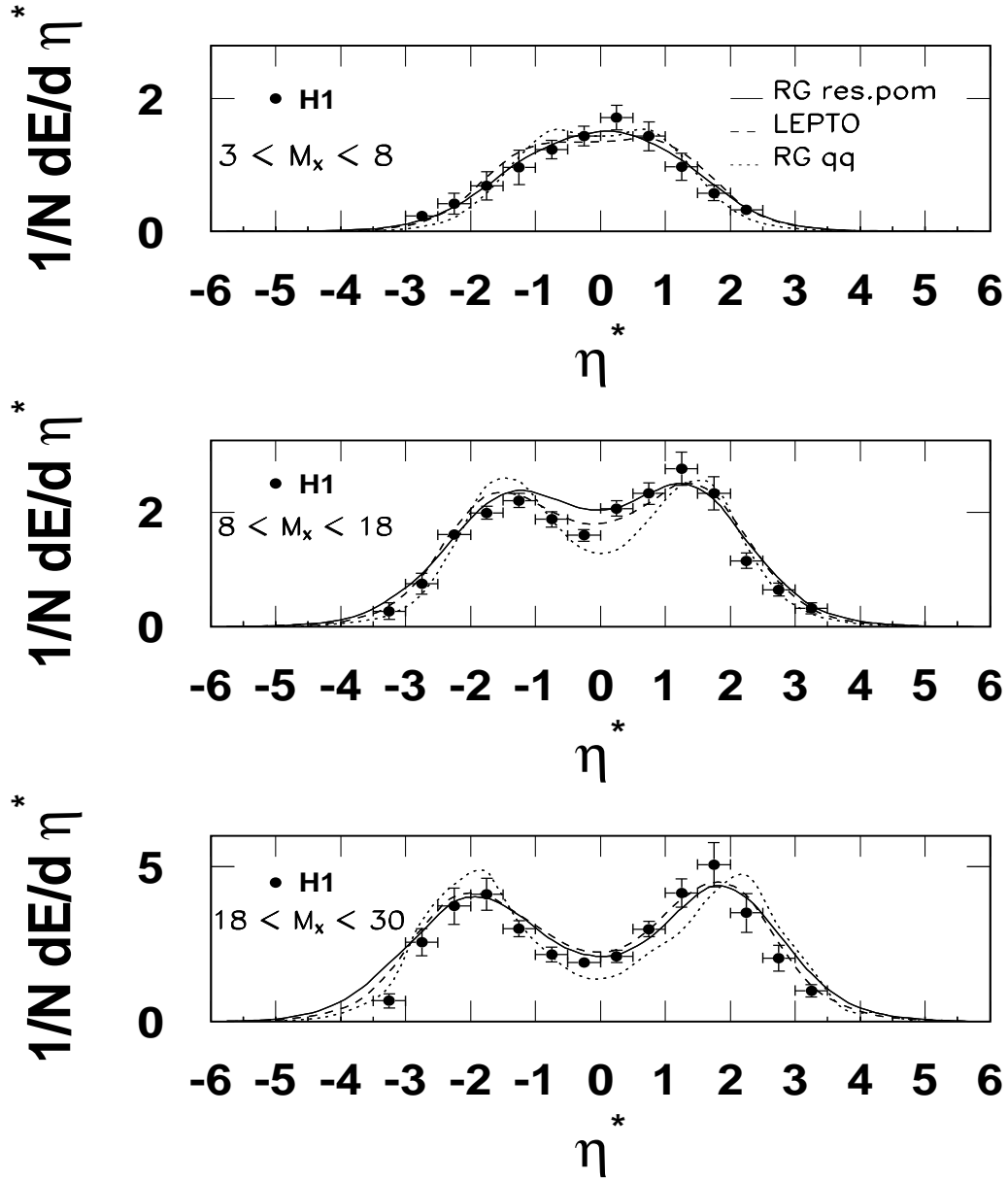


Figure 4: The energy flow in the  $\gamma^*IP$  system  $M_X$  as a function of the pseudo-rapidity in 3 different regions of  $M_X$  (in GeV) indicated as measured by H1 [52]. The solid line is the prediction of RAPGAP in the resolved pomeron mode using fit 2 of the H1 parameterization of  $F_2^{D(3)}$  [51]. The dashed curve is the prediction of LEPTO 6.5 using  $R_{SCI} = 0.5$  with the GRV structure function of the proton. The dotted curve shows the prediction of the perturbative QCD calculation as implemented in RAPGAP.

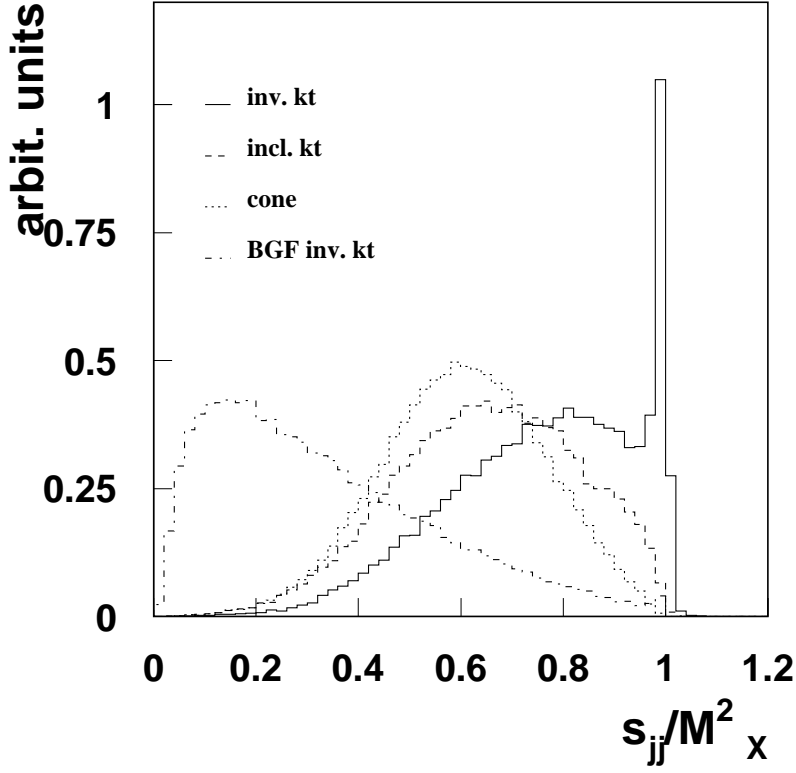


Figure 5: The ratio  $R_{jj} = \hat{s}_{jj}/M_X^2$  of the invariant mass squared of the jet-jet system to the total diffractive mass  $M_X^2$  for exclusive di-jet production according to the pQCD calculation. The solid line is obtained using the  $k_T$  jet algorithm with a  $y_{cut}$  such that two hard jets with  $k_T > 2$  GeV and a possible remnant jet are reconstructed in the Breit frame (labeled inv.  $k_T$ ), the dashed line with the inclusive  $k_T$  jet algorithm and the dotted line with the cone jet algorithm. For comparison the distribution obtained from the resolved  $IP$  model using BGF processes are shown with the dashed-dotted line. Please note that the normalization of the distributions is arbitrary.

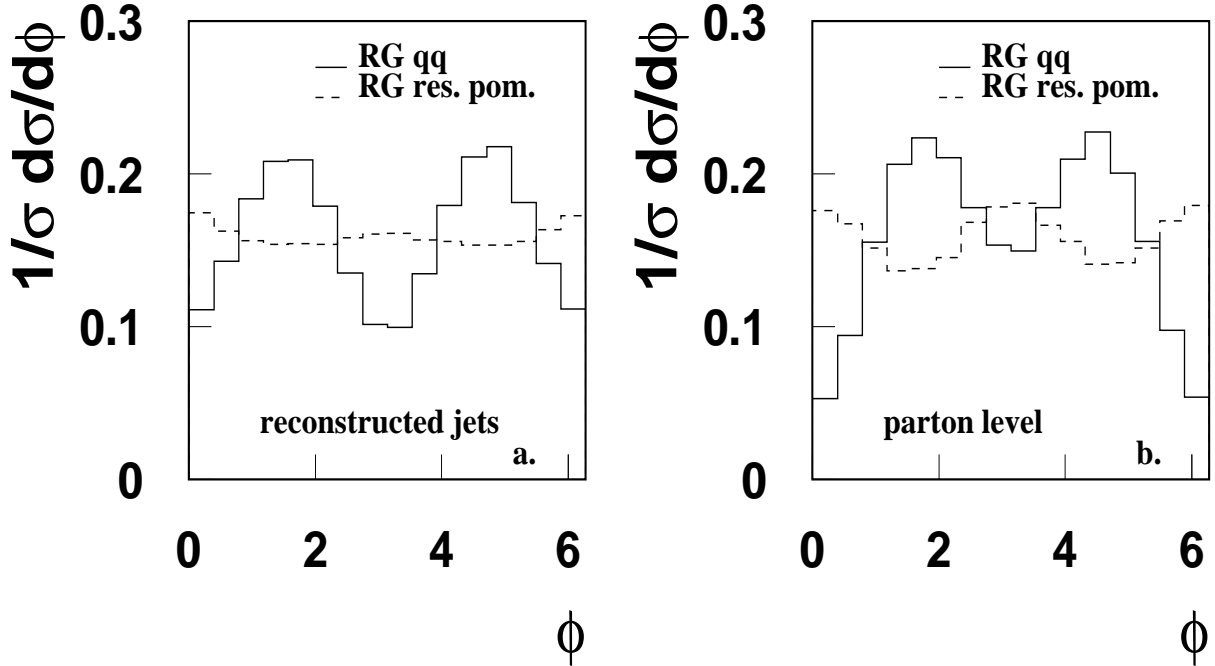


Figure 6: *a.* The  $\phi$  asymmetry of one jet with the electron plane for high  $p_T$  di jet events in the region  $0.1 < y < 0.7$ ,  $5 < Q^2 < 80 \text{ GeV}^2$   $x_P < 0.05$  and  $p_T^{jet} > 2 \text{ GeV}$ . The solid line shows the prediction from the two gluon exchange mechanism after jet reconstruction at the hadron level. The dashed line shows the  $\phi$  dependence from a BGF type process in diffraction (one gluon exchange). In *b.* the  $\phi$  asymmetry of the quark with the electron plane is shown for comparison. The predictions are obtained with the RAPGAP Monte Carlo.

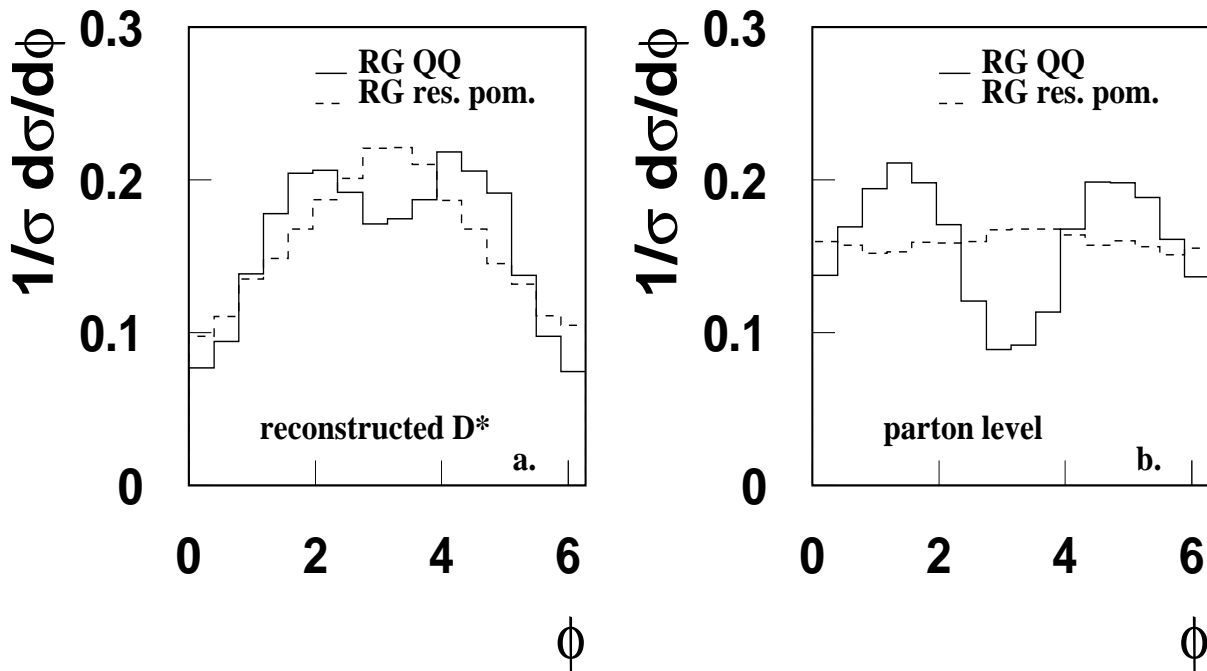


Figure 7: *a.* The  $\phi$  asymmetry of the  $D^*$  jet with the electron plane in the kinematic region  $0.06 < y < 0.6$ ,  $2 < Q^2 < 100 \text{ GeV}^2$ ,  $x_P < 0.05$ ,  $p_T^{D^*} > 1 \text{ GeV}$  and  $|\eta^{D^*}| < 1.25$ . The solid line shows the prediction from the two gluon exchange mechanism after hadronization. The dashed line shows the  $\phi$  dependence from a BGF type process in diffraction (one gluon exchange). In *b* the  $\phi$  asymmetry of the quark with the electron plane is shown. The predictions are obtained with the RAPGAP Monte Carlo.

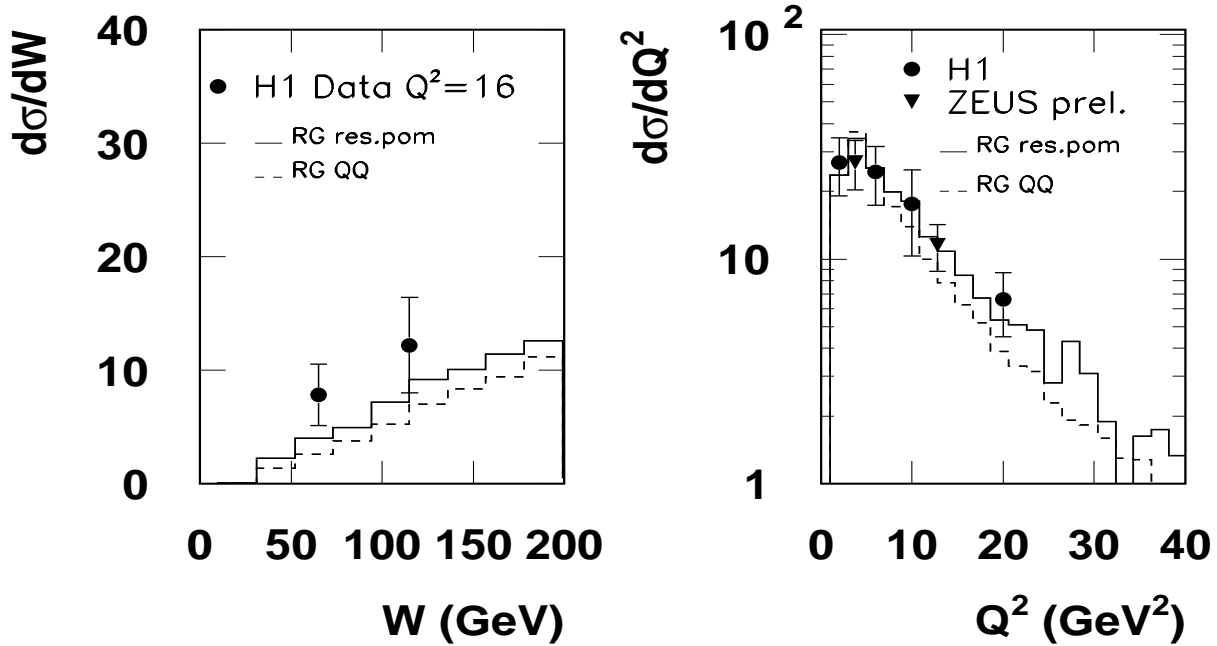


Figure 8: The  $\gamma^*p$  cross section for exclusive  $J/\psi$  production, as a function of  $W$  (a.) and as a function of  $Q^2$  (b.). The solid line is the RAPGAP prediction using the H1  $F_2^{D(3)}$  parameterization [51] (fit 2). The dashed line is the prediction from the pQCD calculation using the model of  $J/\psi$  production described in the text. In all predictions the charm mass was set to  $m_c = 1.5$  GeV. The H1 [58] and ZEUS preliminary [59] data are shown. In b. the points at  $Q^2 < 10$  GeV $^2$  are preliminary H1 data [61].